Ray-tracing simulation and experiment of High Frequency radio wave between McMurdo Station SuperDARN and e-POP during the December 4, 2021 eclipse

Binjie Liu[1], Gareth Perry[1], Joe Huba[2], Lindsay Goodwin[1] and William Bristow[3]

1. Center for Solar-Terrestrial Research, New Jersey Institute of Technology 2. Syntek Technologies 3. Penn State

E-mail: bl395@njit.edu

INTRODUCTION

- High Frequency (HF; 3-30 MHz) radio waves are highly sensitive to plasma density variations in the ionosphere.
- A solar eclipse causes a significant reduction of the plasma temperature and plasma density, leading to a change in HF radio wave propagation conditions (refractive index) in the ionosphere.
- This work presents a raytracing simulation of the Doppler shift of McMurdo SuperDARN transmissions received by the Radio Receiver Instrument (RRI) onboard the e-POP during the December 4 eclipse along with several other measurements from November 29 to December 10 using PHaRLAP based on the ionospheric plasma density generated by the SAMI3 model and compares the predicted HF signal reception characteristics to RRI.
- SAMI3 is a three-dimensional model of the ionosphere/plasmasphere system (Huba et al., 2008) that can be used to study the effect of a solar eclipse on the ionosphere (Huba and Drob, 2017).

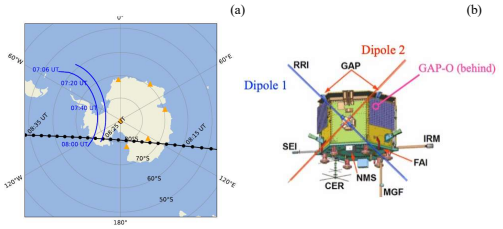

Figure 1 (a) The map above shows the e-POP trajectory (black) and the eclipse path (width of umbra's path in blue). (b) e-POP diagram (Perry et al., 2017) focusing on RRI Dipole 1 measurements.

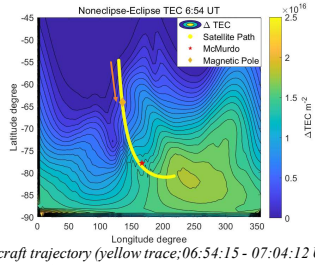

Figure 2 Spacecraft trajectory (yellow trace;06:54:15 - 07:04:12 UT) with background as TEC difference between Eclipse and No Eclipse case. The high TEC area represents the eclipse. The orange arrow shows the direction of the spacecraft. The TEC values are derived from a SAMI3 model.

- ΔTEC is the TEC of No eclipse subtract the TEC of Eclipse.
- The maximum of ΔTEC is approximately 1.8 TECU (1TECU=10^{16} m^{-2}).

OBJECTIVE

Using HF ray-tracing simulations and e-POP observations to study the impact of the December 4, 2021 eclipse on the ionosphere in Antarctica.

METHODOLOGY

- Ray-tracing package: PHaRLAP (Cervera et al., 2014).
- Ionosphere: SAMI3.
- Magnetic field: IGRF 2016 model.
- Ray-trace honing algorithm (James, 2006)
- Transmitting frequency： 10.3 MHz.
- Transmitter location: McMurdo Station (77.8 S 166.7 E)
- Receiver: RRI on board e-POP spacecraft
  Receiving zone is 100 m distance from the spacecraft
- Spacecraft trajectory : Location data with time increment 1 s.
- RRI sampling rate : 62500.33933 Hz

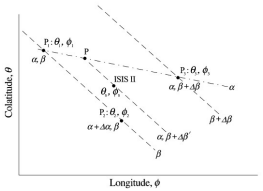

Figure 3 2D interpolation in colatitude and longitude for finding solution rays. Contours of constant azimuth β of starting wave vector are in dashed lines, and one contour of constant elevation angle α is in dot-dash line. (James, 2006)

- Initial elevation angle α and bearing angle β derived from the line of sight between the transmitter and e-POP.
- Initial $\Delta\alpha = 1°, \Delta\beta = 10°$

$$\Delta\alpha' = \Delta\alpha\begin{bmatrix}\phi_s-\phi_1-\left(\frac{\phi_3-\phi_1}{\theta_3-\theta_1}\right)(\theta_s-\theta_1)\\ \phi_2-\phi_1-\left(\frac{\phi_3-\phi_1}{\theta_3-\theta_1}\right)(\theta_2-\theta_1)\end{bmatrix} \quad \Delta\beta' = \Delta\beta\begin{bmatrix}\phi_s-\phi_1-\left(\frac{\phi_3-\phi_2}{\theta_3-\theta_2}\right)(\theta_s-\theta_1)\\ \phi_3-\phi_1-\left(\frac{\phi_3-\phi_2}{\theta_3-\theta_2}\right)(\theta_3-\theta_1)\end{bmatrix}$$

- In general, after 10 iterations, the distance between the ray and e-POP converges to a constant which may not be inside the receiving zone.
- If the converged distance is not within 100 m, then use the corresponding α and β as new initial condition, use random $\Delta\alpha$ and $\Delta\beta$ between 0° and 1° to start a new iteration.
- This procedure is repeated until a ray reaches the receiving zone. If no ray reaches the receiving zone after 20 the procedure is repeated times is regarded as not received.
- We assume that during the spacecraft conjunction the ionosphere and the radar radiation pattern are fixed.
- The received Doppler shift can be expressed in frequency as (Ponomarenko et al., 2009).

$$\boldsymbol{\Delta f = -\frac{1}{\lambda_0}\left[\frac{\partial}{\partial t}\int_A^{B(t)} nds + \frac{\partial B(t)}{\partial t}n(B)\right]} \qquad (1)$$

- λ_0 is the wavelength of 10.3 MHz in meters, n is the refractive index, B is the location of the receiver (e-POP here), A is the location of transmitter (McMurdo SuperDARN), ds is the differential path length.
- Equation (1) can be re-expressed as:

$$\boldsymbol{\Delta f = -\frac{n}{\lambda_0}\frac{\partial(P_{receive})}{\partial t}} \qquad (2)$$

- $\boldsymbol{P_{receive}}$ is the phase path at receiving point.
- In order to illustrate the effect of eclipse to the ionosphere in e-POP observation data, we select data on December 7, 2021 as the non-eclipse reference.

RESULTS

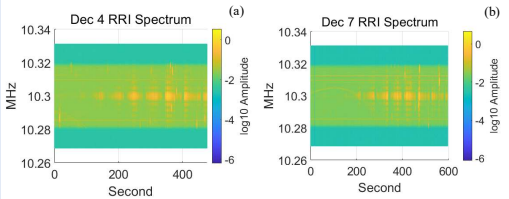

Figure 4 The RRI dipole 1 observation spectrum for eclipse and non-eclipse case. Color-coded with log10 of normalized amplitude(a) is for the e-POP trajectory Dec 4, 2021, 06:54:15-07:04:12 UT; (b) is for trajectory Dec 7, 2021, 06:54:14 UT -07:04:11 UT.

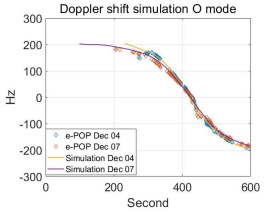

Figure 5 Doppler shift of observation result of the two trajectories and 8th order polynomial fit of O mode simulation for eclipse and no eclipse conjunctions. The central frequency is 10.3 MHz.

- Horizonal axis is the elapsed time in seconds during the conjunction.
- The Doppler maximum error in simulation is approximately 3 Hz at 10.3 MHz signal caused by 100 m receiving zone.
- With high accuracy raytracing result, the simulation matches observation well.
- There is mismatch between simulation and observation prior 297 second on Dec 4 conjunction due to low elevation angle.
- The maximum variation between simulation and observation Doppler on Dec 7 conjunction is about 10 Hz and 4 Hz on Dec 4 conjunction after 297 second.
- Simulation shows more receiving signals at low elevation angle than e-POP observation data.

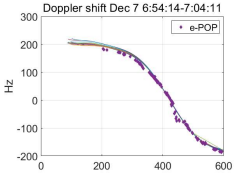

Figure 6 Doppler shift of simulation with SAMI3 ionosphere 0 to 23 UT on Dec 7 with 3-hour increment for the same e-POP conjunction. Time period shown in the title in UT.

- The ionosphere used in Figure 5 for Dec 7 conjunction is SAMI3 at 7:00 UT.
- Electron density variation in the ionosphere could be detected in the Doppler frequency aspect shown in Figure 6.

DISCUSSION

Date	Conjunction time UT	Number of pulses Doppler difference larger than 10Hz	e-POP signal pulse number	Percentage %
Nov 29	06:25:15-06:33:12	0	27	0
Nov 30	07:33:15-07:41:12	5	150	3.33
Dec 1	07:00:15-07:06:12	0	122	0
Dec 3	07:35:15-07:41:12	4	55	7.27
Dec 4(eclipse)	06:54:15-07:04:12	7	203	3.45
Dec 5	06:21:15-06:29:12	30	273	10.99
Dec 7	06:54:14-07:04:11	8	224	3.57
Dec 8	06:21:14-06:29:11	9	145	6.21
Dec 9	09:10:14-09:20:11	11	108	10.18
Dec 10	06:55:14-07:03:11	2	107	1.87
Dec 11	06:21:14-06:29:11	3	91	3.29

- This table shows a statistical result of the reliability of ray tracing simulation on Doppler frequency with SAMI3 ionosphere for ten e-POP observations over 13 days time span.
- First two columns is the time of observation periods
- Third column is the number of observed signal pulse peaks when their Doppler difference between simulation and observation larger than 10 Hz.
- Fourth column is the total observed signal pulse peaks during each conjunction
- Simulation error caused by size of receiving zone is approximately 3 Hz. The statistical result shows among 10 conjunctions, less than 10% of data points when the difference between simulation and observation larger than 10Hz (except for Dec 5th and 9th).

CONCLUSION AND FUTURE WORK

- Ray tracing simulation under SAMI3 ionosphere has strong reliability in Doppler frequency detection between McMurdo and e-POP spacecraft.
- e-POP RRI is sensitive enough to pick up tens Hz variation in frequency from SuperDARN transmitted signal.
- The ray tracing algorithm with Newton's iteration significantly improves the compute efficiency and accuracy. It does not require high level hardware in computing.
- Further work will include deriving the TEC between McMurdo SuperDARN and e-POP spacecraft by using the RRI Doppler data.

REFERENCES

Cervera, M. A., & Harris, T. J. (2014). Modeling ionospheric disturbance features in quasi-vertically incident ionograms using 3-D magnetoionic ray tracing and atmospheric gravity waves. Journal of Geophysical Research: Space Physics, 119(1), 431-440.

Weber, E. J., Buchau, J., Moore, J. G., Sharber, J. R., Livingston, R. C., Winningham, J. D., & Reinisch, B. W.(1984). F layer ionization patches in the polar cap. Journal of Geophysical Research: Space Physics, 89(A3), 1683-1694.

Perry, G. W., James, H. G., Gillies, R. G., Howarth, A., Hussey, G. C., McWilliams, K. A., Yau, A. W. (2017). First results of HF radio science with e-POP RRI and SuperDARN. *Radio Science*, *52*(1), 78–93. https://doi.org/10.1002/2016RS006142

Ponomarenko, P. V., St-Maurice, J. P., Waters, C. L., Gillies, R. G., & Koustov, A. V. (2009, November). Refractive index effects on the scatter volume location and Doppler velocity estimates of ionospheric HF backscatter echoes. In Annales Geophysicae (Vol. 27, No. 11, pp. 4207-4219). Copernicus GmbH.

Huba, J. D., Joyce, G., & Krall, J. (2008). Three-dimensional equatorial spread F modeling. Geophysical Research Letters, 35(10).

Huba, J. D., Maute, A., & Crowley, G. (2017). SAMI3_ICON: Model of the ionosphere/plasmasphere system. Space science reviews, 212(1), 731-742.

James, H. G. (2006). Effects on transionospheric HF propagation observed by ISIS at middle and auroral latitudes. Advances in Space Research, 38(11), 2303-2312.

Acknowledgements

The authors acknowledge the use of SuperDARN data. SuperDARN is a collection of radars funded by national scientific funding agencies of Australia, Canada, China, France, Italy, Japan, Norway, South Africa, United Kingdom and the United States of America

This work is supported by NASA Award # 80NSSC21K1774